Influence of rain on polarimetric detection of wet road surfaces: an experimental evaluation under simulated rain conditions

Mouhamadou Makhtar Fall[a], Samia Ainouz[a], Pierre-Jean Lapray[b], and Jean-Philippe Tarel[c]

[a]LITIS Laboratory, INSA Rouen Normandie, Univ Rouen Normandie, Normandie Univ, F-76000 Rouen, France
[b]IRIMAS-UR7499, Université de Haute-Alsace, Mulhouse, France
[c]COSYS-PICS-L, Univ Gustave Eiffel, F-77454 Marne-la-Vallée, France

ABSTRACT

Detecting the surface condition of roads is a key challenge for assisted and autonomous navigation systems, particularly at night or under adverse weather conditions where the loss of adhesion drastically increases the risk of accidents. Conventional vision or lidar-based methods often fail to accurately estimate road wetness or slipperiness when visibility is degraded, as they rely mainly on intensity or depth cues that are highly sensitive to illumination and scattering effects. In this context, polarimetric imaging offers a promising alternative by exploiting the polarization state of reflected light to extract information about surface properties, even in the presence of disturbing reflections or scattering media. This study evaluates the capability of polarimetric imaging to discriminate between different road surface states under various rainfall conditions and illumination sonditions. We analyze the backscattering behavior of wet surfaces in a scattering environment and compare the performance of two illumination types: polarized and non-polarized light. Experiments were conducted on the CEREMA PAVIN2 platform designed for rainfall simulation, covering several scenarios (dry surface, light rain, moderate rain, heavy rain, and water film). The polarimetric camera effectively suppresses parasitic reflections from ambient light, and the use of polarized illumination enhances discrimination between rainfall levels. These findings confirm the relevance of polarimetric imaging for reliable road surface estimation, especially for autonomous and assisted vehicles operating at night or in degraded weather conditions.

Keywords: polarimetric imaging, road surface state estimation, scattering media, polarization contrast, optical sensing

1. INTRODUCTION

Road safety remains a major concern worldwide, with a significant proportion of accidents caused by reduced tire–road adhesion, particularly under adverse weather conditions. Wet pavement surfaces, combined with low visibility at night, create hazardous driving scenarios where vehicle skidding becomes more likely. Advanced Driver-Assistance Systems (ADAS) and autonomous vehicles rely heavily on accurate perception modules to detect and respond to such conditions in real time. Among the sensors deployed in these systems, cameras are widely used for their low cost and rich spatial information, yet they often struggle to reliably characterize road surface states under challenging illumination or rainfall scenarios. Active sensing technologies such as LiDAR or radar can complement optical systems,[1] but they remain costly, computationally demanding, and are not specifically designed to directly characterize pavement surface conditions.

Early approaches to road surface detection relied on RGB image-based texture analysis[2] or deep learning classifiers,[3] but these methods exhibit clear limitations in the presence of water films and specular reflections that

Further author information: (Send correspondence to Samia Ainouz)
Mouhamadou Makhtar Fall: E-mail: mouhamadou.fall@insa-rouen.fr
Samia Ainouz: E-mail: samia.ainouz@insa-rouen.fr, Telephone: +33 (0)2 32 95 66 27
Pierre-Jean Lapray: E-mail: pierre-jean.lapray@uha.fr, Telephone: +33 (0)3 89 33 69 58
Jean-Philippe Tarel: E-mail: jean-philippe.tarel@univ-eiffel.fr, Telephone: +33 (0)1 81 66 83 71

degrade perception reliability. In this context, polarimetric imaging has emerged as a promising alternative.[4] By analyzing the polarization state of reflected light, it becomes possible to suppress fog,[5,6] enhance contrast, and extract surface properties that are invisible to standard imaging sensors. Yamada et al.[7] pioneered this direction by demonstrating that polarization cues could discriminate between dry, wet, and icy road surfaces, and later extended their approach to vehicle-mounted systems under real driving conditions.[8] Casselgren et al.[9] evaluated polarized infrared prototype systems, achieving classification accuracies of 80–95% across dry, wet, icy, and snowy surfaces, while also highlighting that polarization differences alone may be insufficient for robust estimation without additional surface features. Ryu et al.[10] combined polarization analysis with wavelet-based texture features, demonstrating robust multi-class road condition classification using only camera images. More recently, Blin et al.[11] proposed a dedicated polarimetric dataset for road scene analysis and demonstrated the benefit of polarimetric cues for object detection under various illumination conditions, opening the door to low-cost wide-area monitoring.

Despite these advances, most existing studies remain limited to controlled environments or daytime scenarios, and few address the combined effect of nighttime illumination and active rainfall on the polarimetric response of the pavement. In particular, the influence of rain intensity on key polarimetric descriptors such as the Degree of Linear Polarization (DoLP) and the Angle of Polarization (AoP) has not been systematically investigated.

In this work, we characterize the evolution of polarimetric signature statistics under varying illumination levels, road surface states and rainfall intensities using the CEREMA PAVIN2 platform. Two illumination configurations are compared: conventional unpolarized illumination, and vertically polarized light . Height surface conditions are considered, ranging from dry pavement to six rainfall intensities (17 to 300 mm/h). We analyze line-wise statistics of S_0, DoLP, and AoP dispersion to characterize how polarimetric signatures evolve with rainfall intensity and viewing geometry.

The remainder of this paper is organized as follows. Section 2 presents the experimental platform, imaging system, and dataset acquisition protocol. Section 3 describes the polarimetric processing pipeline and the line-wise metrics applied to processed data. Section 4 reports and discusses the experimental results. Finally, Section 5 concludes the paper and outlines future perspectives.

2. EXPERIMENT AND DATASET DESCRIPTION

2.1 Experimental Platform

Experiments were conducted on the PAVIN2 platform (see Figure 1), an adverse-weather simulation facility developed by Cerema.[12] This platform is specifically designed to reproduce controlled and repeatable environmental conditions such as rain and fog for the evaluation of sensing systems.

The facility consists of a covered test track approximately 50 m long, 5 m wide, and 5 m high, allowing dynamic experiments under realistic yet controlled conditions. One of the key features of the platform is the full control of illumination, including both artificial lighting and natural light contributions, enabling consistent acquisition conditions across experiments.

The platform is equipped with systems for generating homogeneous and stable fog, with adjustable meteorological visibility ranging from 10 m to 1000 m. In addition, a rainfall generation system allows precise control of precipitation intensity, covering a wide range from 16 to 300 mm/h, from light rain to heavy precipitation.

This controlled environment makes the platform particularly suitable for studying the impact of adverse weather conditions on polarimetric imaging of road surfaces, as it enables the isolation of rainfall effects while ensuring high repeatability of the measurements .

2.2 Imaging System

The imaging system consisted of a Lucid Vision Labs TritonT TRI050S1-QC polarimetric color camera equipped with a Sony IMX264MYR sensor. This camera captures four polarization angles simultaneously (0°, 45°, 90°, 135°) based on a division-of-focal-plane architecture,[13] using a micro-polarizer array integrated directly on the sensor, with a resolution of 2448 × 2048 pixels (≈5 MP) and a frame rate of up to 50 fps at full resolution. Its high dynamic range and color fidelity make it well suited to low-light and nighttime conditions.



Figure 1. CEREMA PAVIN2 platform for extreme and controlled weather generation in Clermont-Ferrand, France.

The camera was mounted on a tripod at a 25° inclination relative to the vertical axis, mimicking the viewpoint of a vehicle-mounted sensor while maintaining sensitivity to both diffuse and specular reflections from the pavement (Figure 2).

2.3 Illumination and Acquisition Protocol

Illumination was provided by two light sources positioned above the camera. The first source was equipped with a linear polarizing filter mounted on a rotating holder; in this study, only the vertical polarization orientation was used, as it produces the strongest contrast between dry and wet surfaces at the considered viewing angle. The second source emitted unpolarized light, simulating conventional illumination conditions.

For each surface condition, including dry pavement, fully wet pavement without rainfall, and six rainfall levels (17, 40, 60, 125, 194, and 300 mm/min), image sequences were acquired under both polarized and unpolarized illumination. This protocol ensures that all combinations of surface state and illumination type are systematically captured under identical environmental conditions, allowing a direct comparison of the two illumination modes. Each scenario contains approximately 20 to 30 images, depending on the acquisition sequence. The resulting dataset samples are illustrated in Figure 3



Figure 2. Experimental setup at the CEREMA PAVIN2 platform. The polarimetric camera is mounted at 25° inclination above the pavement. The two light sources (polarized and unpolarized) are positioned above the scene to simulate nighttime driving illumination conditions.



Figure 3. Examples of pavement images acquired under different surface and illumination conditions (green channel). Top row: vertically polarized illumination. Bottom row: unpolarized illumination. From left to right: dry surface, moderate rain (60 mm/h), and heavy rain (300 mm/h).

3. DATA PROCESSING AND METRICS

This section describes the processing pipeline applied to the raw camera data to extract polarimetric descriptors and derive line-wise metrics that characterize the influence of rainfall on the pavement response (Figure 4). The pipeline consists of two stages: (i) the computation of physically meaningful polarimetric quantities from the raw sensor output, and (ii) the extraction of row-level statistics that relate these quantities to viewing geometry and surface condition.

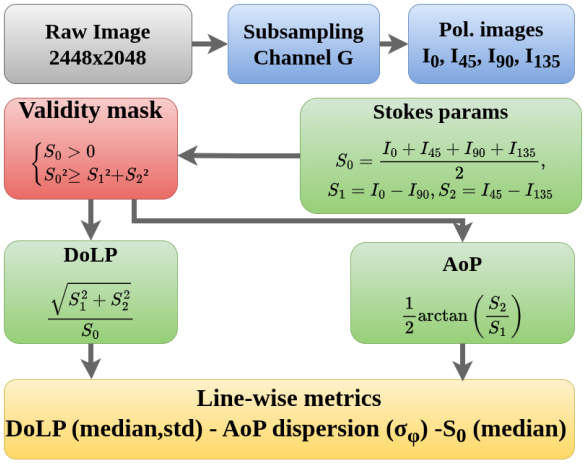


Figure 4. Processing pipeline: from raw sensor output to line-wise polarimetric metrics.

3.1 Subsampling and Channel Selection

The sensor delivers a single raw image in which each 4×4 superpixel contains pixels sensitive to four polarization angles (0°, 45°, 90°, 135°) and three color channels (R, G, B), following the layout of the Sony IMX264MYR micro-polarizer array. Demosaicking is performed by extracting, for each polarization angle and each superpixel, the corresponding color channel intensity. For the green channel, two green-sensitive pixels are available per superpixel; their average is used to reduce noise:

$$I_\theta^G = \frac{1}{2}\left(p_\theta^{G,1} + p_\theta^{G,2}\right), \quad \theta \in \{0°, 45°, 90°, 135°\}, \tag{1}$$

where $p_\theta^{G,k}$ denotes the k-th green pixel at polarization angle θ within the superpixel.

Only the green channel is retained for all subsequent analyses. This choice provides a favorable trade-off between sensor sensitivity under artificial illumination and polarimetric contrast, while avoiding chromatic artifacts that can arise when combining multiple spectral bands. The output of this stage is a set of four intensity images I_0, I_{45}, I_{90}, I_{135} of reduced resolution (612×512 pixels).

3.2 Stokes Parameters and Polarimetric Quantities

For partially polarized light, the transmitted intensity through a linear polarizer at angle θ can be decomposed into a polarized and an unpolarized component:

$$I(\theta) = \frac{I_{\text{unpol}}}{2} + I_{\text{pol}} \cos^2(\theta - \phi), \tag{2}$$

where I_{unpol} is the intensity of the unpolarized component, I_{pol} is the intensity of the linearly polarized component, and ϕ is the angle of polarization (AoP) of the incident light.

From the four demosaicked images, the first three Stokes parameters are computed pixel-wise as:

$$S_0 = \frac{I_0 + I_{45} + I_{90} + I_{135}}{2}, \tag{3}$$

$$S_1 = I_0 - I_{90}, \tag{4}$$

$$S_2 = I_{45} - I_{135}, \tag{5}$$

where S_0 represents the total intensity, and S_1, S_2 encode the linear polarization state. A validity mask is applied prior to computing derived quantities, retaining only pixels that satisfy the physical constraint $S_0 > 0$ and $S_0^2 \geq S_1^2 + S_2^2$; pixels outside this mask are not considered in the computation.

The Degree of Linear Polarization (DoLP) and the Angle of Polarization (AoP) are then derived as:

$$\text{DoLP} = \frac{\sqrt{S_1^2 + S_2^2}}{S_0}, \tag{6}$$

$$\phi = \frac{1}{2}\arctan\left(\frac{S_2}{S_1}\right). \tag{7}$$

DoLP quantifies the fraction of linearly polarized light (DoLP $\in [0, 1]$), while AoP gives the angle of the major axis of the palarization ellipse in the image plane. These quantities are sensitive to surface properties such as roughness, water-film thickness, and scattering by falling raindrops, and therefore provide discriminative cues to separate dry and wet road states under different rainfall intensities.

3.3 Line-wise Metrics

Because the camera is tilted with respect to the pavement, image rows approximately correspond to increasing distances from the sensor along the road plane. This geometric configuration was also used with advantages for meteorological visibility estimation from road images.[14] The road region of interest (ROI), shown in Figure 5, is first manually defined for each configuration and then used to extract line-wise statistics of the polarimetric quantities. This representation makes it possible to relate the evolution of polarization and intensity signatures to both viewing geometry and rainfall intensity.

Angular dispersion of the AoP. The Angle of Polarization ϕ is a circular variable defined modulo π, which makes classical statistics such as a linear mean or standard deviation inappropriate. To obtain a robust measure of its variability along each image row, we compute use directional or circular statistics.[15]

For a given row within the pavement ROI, the AoP values $\{\phi_k\}_{k=1}^{N}$ are first mapped to doubled angles $2\phi_k$ in order to account for the π-periodicity of linear polarization. Following circular statistics, the mean resultant vector is obtained as:

$$C = \frac{1}{N}\sum_{k=1}^{N}\cos(2\phi_k), \tag{8}$$

$$S = \frac{1}{N}\sum_{k=1}^{N}\sin(2\phi_k), \tag{9}$$

$$R = \sqrt{C^2 + S^2}, \tag{10}$$

where $R \in [0, 1]$ is the length of the mean resultant vector. From,[15] the *angular dispersion* is defined as half of the circular standard deviation of the AoP for that row:

$$\sigma_\phi = \frac{1}{2}\sqrt{-2\ln(R)}. \tag{11}$$

Low values of σ_ϕ indicate a coherent polarization orientation (e.g., specular reflection from a smooth or uniformly wet surface), whereas high values reflect strong angular fluctuations caused by increased surface roughness, inhomogeneous water films, or rain-induced scattering.

Line-wise DoLP and S_0 statistics. To characterize how the polarization level and total intensity evolve with distance and rainfall, we compute, for each image row inside the pavement ROI, the median and standard deviation of both DoLP and S_0. For the DoLP, the *median* provides a robust central tendency less affected by isolated specular highlights or measurement noise, while the *standard deviation* quantifies local variability induced by texture, micro-geometry of the pavement, water-film inhomogeneities, and raindrops. For S_0, the *median* describes the typical brightness level along the row, mainly driven by illumination geometry, pavement reflectance, and water-film thickness, while the *standard deviation* reflects local contrast and intensity variations due to surface texture and rain-induced highlights. Together, these line-wise profiles constitute the primary family of metrics used to assess the impact of rainfall intensity and illumination polarization on the pavement response, and are particularly useful to reveal how increasing rainfall modifies both the polarimetric state and the specular reflection geometry of the surface. A singular behavior is observed in the spatial evolution of the Aop dispersion compared to other polarimetric descriptors. While intensity-based metrics and DoLP exhibit monotonic trends, the AoP demonstrates opposing derivative signs with respect to distance depending on the road state (dry vs. wet/raining). But this angular sensitivity suggests that the AoP derivative could serve as a signature of the condition transition between dry and rain/wet.

Together, the AoP angular dispersion, the line-wise DoLP statistics, and the line-wise S_0 statistics provide a compact yet expressive set of metrics that summarize the spatial evolution of polarimetric and intensity signatures for different road surface conditions and illumination modes. These metrics are exploited in the next section to analyze the effect of rainfall intensity and polarized illumination on the discriminability between dry and wet road states.

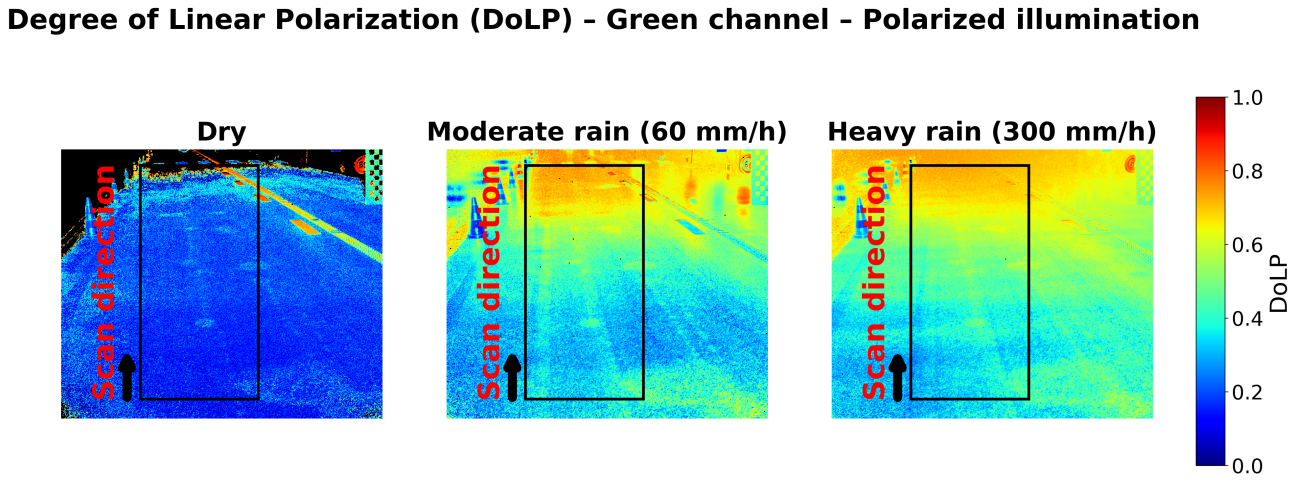
Temporal aggregation. For each experimental scenario, all metrics are first computed on a frame-by-frame basis. For each image row, the corresponding statistics (AoP angular dispersion, DoLP median and standard deviation, and S_0 median and standard deviation) are then averaged over the full sequence. This yields a temporally averaged profile that characterizes the steady-state polarimetric response of the pavement for a given rainfall intensity and illumination condition. Such averaging mitigates frame-to-frame variability induced by stochastic effects such as raindrop impacts and measurement noise.

4. RESULTS AND ANALYSIS

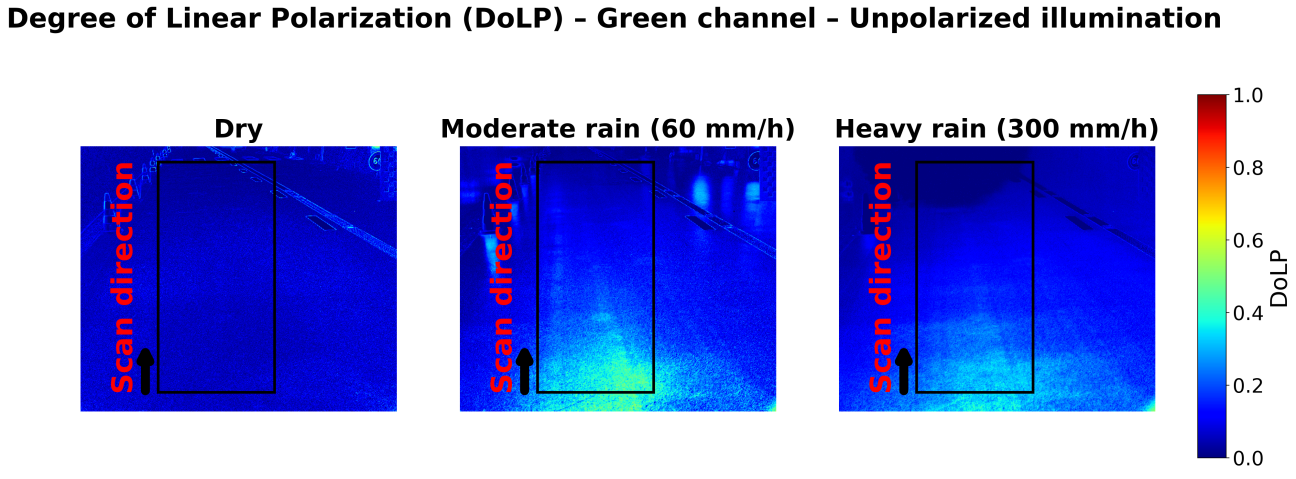
This section presents the experimental results obtained from the line-wise analysis described in Section 3. We first investigate the impact of illumination polarization on the DoLP profiles (Section 4.1), then analyze the effect of rainfall intensity on S_0 and AoP dispersion (Section 4.2), and finally discuss the discriminability between surface states (Section 4.3).

4.1 Effect of Polarized vs. Unpolarized Illumination on DoLP

Figure 5 shows the DoLP maps for three representative surface conditions (dry, moderate rain, and heavy rain) under polarized and unpolarized illumination. Invalid pixels, where the physical constraint $S_0^2 \geq S_1^2 + S_2^2$ is not satisfied, are shown in black. These maps provide a qualitative overview of how the spatial distribution of polarization changes with rainfall intensity and illumination type, before the quantitative line-wise analysis presented in Figure 6.



(a) Polarized illumination



(b) Unpolarized illumination

Figure 5. DoLP maps (green channel) for dry surface, moderate rain (60 mm/h), and heavy rain (300 mm/h). Top row: vertically polarized illumination. Bottom row: unpolarized illumination. Invalid pixels are shown in black.

Figure 6 reports the line-wise statistics of the DoLP for all surface conditions, under both polarized and unpolarized illumination. Each curve corresponds to a given rainfall intensity, and the horizontal axis approximately encodes the distance from the camera along the road plane.

Under polarized illumination, the median DoLP exhibits a globally increasing trend with distance for all rainfall levels, with the clearest separation between rain intensities observed in an intermediate range of rows (roughly corresponding to mid-range distances on the road). In this zone, the viewing geometry favors reflection configurations in which the electric field is strongly aligned with the analyzer direction, so that both the level and the gradient of the median DoLP are highly sensitive to the amount of water on the surface. As a result, the median DoLP profiles form families of curves that rise with distance and are progressively shifted according to rainfall intensity. Interestingly, the wet road condition without active rainfall exhibits lower DoLP values compared to rainy conditions, suggesting that the presence of falling raindrops is associated with lower depolarization than a static water film. This behavior indicates that dynamic conditions may preserve or even enhance the polarization state of reflected light, whereas a homogeneous water layer tends to increase depolarization through multiple scattering and microscale surface effects.

In contrast, under unpolarized illumination, the median DoLP tends to display the opposite trend: the degree of polarization generally decreases with distance, and the curves associated with different rainfall levels are much closer in the distance range where polarized illumination provides strong separation. Since the incoming light is not pre-polarized, the effective polarized component observed by the camera mainly results from reflection and scattering processes at the surface and within the rain volume; these mechanisms become weaker and more diffuse with distance, leading to lower median DoLP values and weaker discrimination between surface states.

The line-wise standard deviation of the DoLP is particularly informative in the polarized configuration. For a given distance, higher rainfall intensities tend to produce lower DoLP variability, indicating that the DoLP values along the row become more homogeneous. This effect can be interpreted as follows: when the rain is intense, the combination of a more uniform water film and a large number of droplets leads to a more consistent polarization state at the scale of the row, which in turn results in a smaller spread of DoLP values. For light rain or dry conditions, the absence of a continuous film and the dominance of small-scale surface features create more heterogeneous polarization patterns and thus higher DoLP standard deviation. This interpretation is further supported by the wet road condition without active rainfall, which also exhibits relatively high DoLP standard deviation. The absence of dynamic raindrops in this scenario prevents the formation of a consistently aligned polarization state, confirming that falling rain contributes to homogenizing the DoLP along the row.

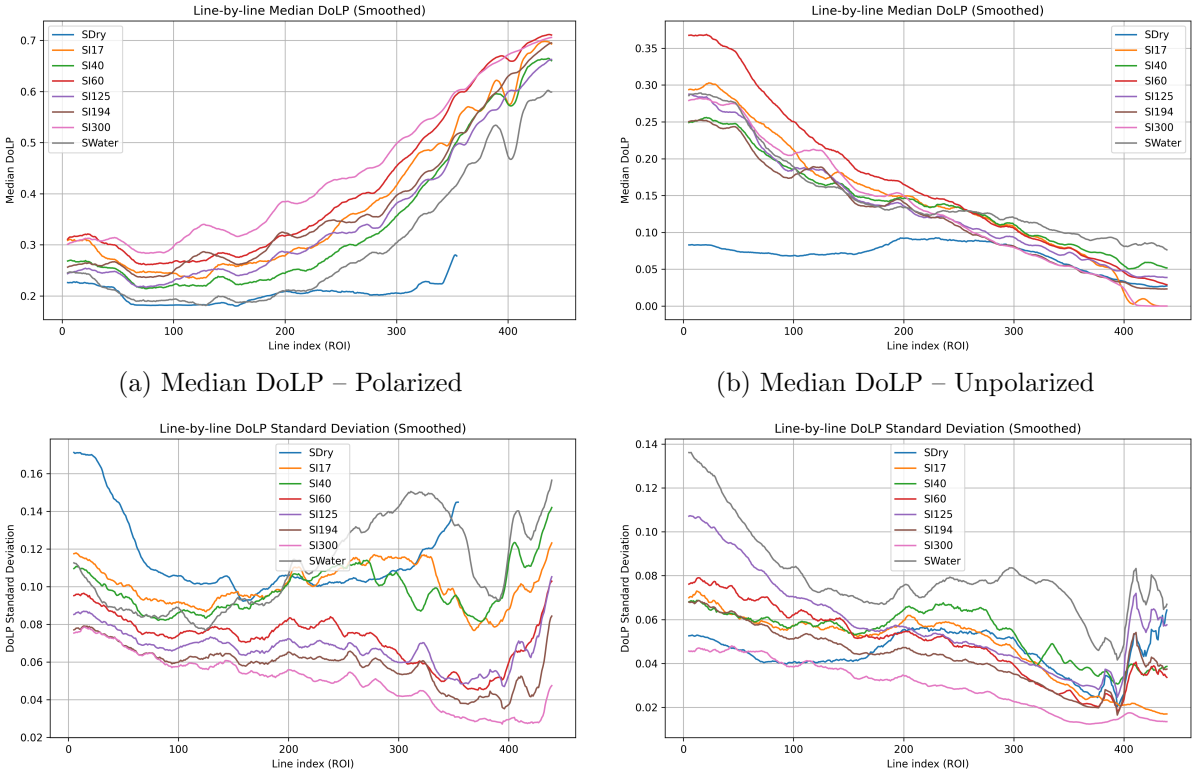
Under unpolarized illumination, the standard deviation of the DoLP shows much less structured behavior across rainfall levels. The curves corresponding to different rain intensities are often intertwined, and the differences are not as clearly linked to the amount of water on the surface. This confirms that the combination of polarized illumination and polarimetric imaging is required to obtain DoLP statistics that are both interpretable and strongly correlated with the rainfall regime.

4.2 Effect of Rainfall Intensity on S_0 and AoP Dispersion

Figure 7 illustrates the line-wise evolution of the median total intensity S_0 for all surface conditions, under polarized and unpolarized illumination. In the polarized case, the camera response is highly consistent: in the central part of the image, where the signal-to-noise ratio is high and the geometry is favorable, the median S_0 increases monotonically with rainfall intensity. This trend reflects the fact that S_0 combines two main contributions: the specular and diffuse return from the wet road surface, and the backscattered light coming from the falling droplets. As the rainfall intensity grows, the water film thickens and the number of illuminated droplets increases, leading to higher total intensity in this distance range. Very close to the camera and at large distances, the profiles can be more affected by local saturation or noise, but the global ordering of the curves with respect to rain level remains stable.

Under unpolarized illumination, the behavior of S_0 is more sensitive to the presence of water, and strong peaks may appear in the profiles. The wet surface and the droplets can produce intense specular highlights that lead to very high local values of S_0, potentially causing glare and saturation in the camera. This effect makes the intensity-only interpretation more fragile, since small changes in rainfall or illumination conditions can trigger large variations in brightness and reduce the robustness of an intensity-based detection.

The impact of rainfall on the angular dispersion of the AoP is summarized in Figure 8. For the dry surface, the dispersion takes relatively high values over large parts of the road, which is consistent with the rough



(a) Median DoLP – Polarized

(b) Median DoLP – Unpolarized

(c) DoLP Std – Polarized

(d) DoLP Std – Unpolarized

Figure 6. Line-by-line statistical analysis of the Degree of Linear Polarization (DoLP) for different road surface conditions. Left column: polarized illumination. Right column: unpolarized illumination. The median captures the robust central polarization trend, while the standard deviation reflects spatial variability induced by rainfall and surface water films.

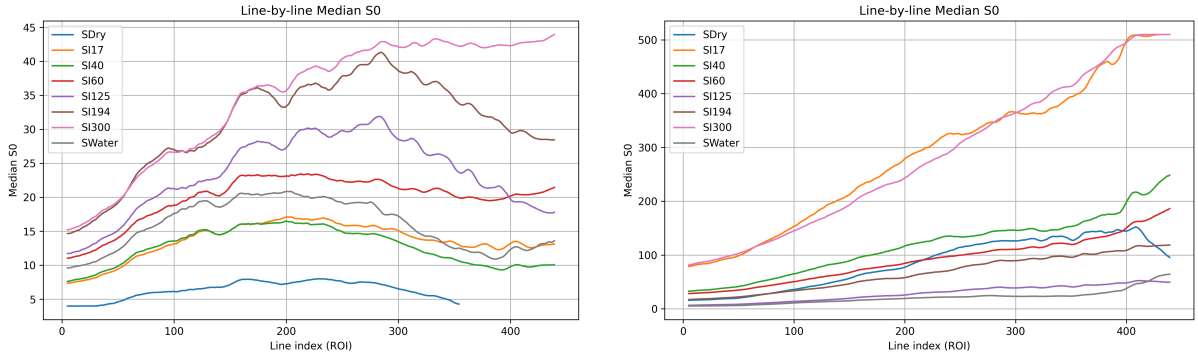
micro-geometry of the asphalt and the absence of a continuous water film. In this regime, many different facet orientations contribute to the reflected signal, and the polarization direction varies significantly from pixel to pixel.

When rainfall increases and a water film starts to cover the pavement, the AoP dispersion decreases markedly in the same intermediate distance range where DoLP and S_0 show the strongest rain-dependent variations. The water layer partially smooths the effective optical interface and reduces the influence of the underlying roughness, so that the dominant reflection geometry becomes more uniform within a row. In addition, the scattering by droplets tends to polarize the light in similar directions for neighboring pixels, which further contributes to the reduction of angular dispersion.

A similar trend is observed under unpolarized illumination, but the effect is more pronounced when the scene is illuminated by polarized light. In the polarized configuration, the initial polarization state is well defined, so any alignment or smoothing induced by the water film and raindrops translates into a clear decrease of AoP dispersion. This makes the angular dispersion metric especially valuable for distinguishing dry, moderately wet, and heavily wet conditions in the polarized case.

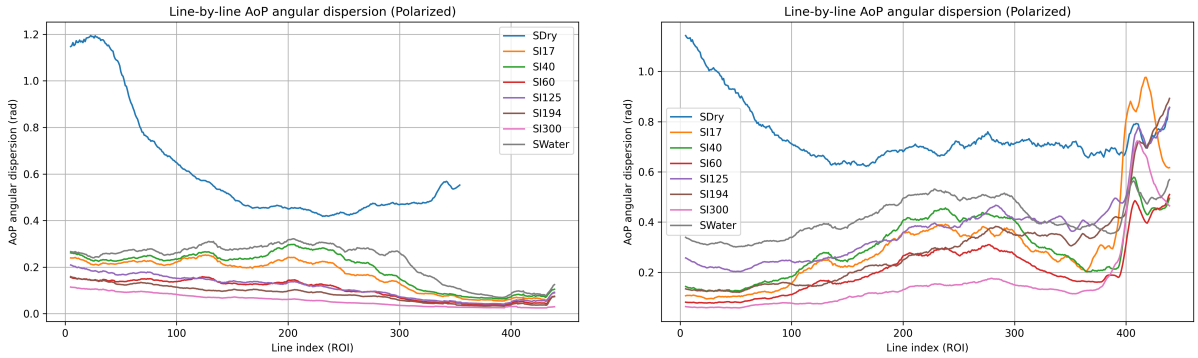
4.3 Discriminability Between Surface States

The joint analysis of DoLP, S_0, and AoP dispersion provides insights into the discriminability between the different pavement surface conditions considered in this work. From Figure 6, one can identify a band of image rows in the middle of the field of view where the median DoLP curves corresponding to distinct rainfall intensities are clearly separated under polarized illumination, while they remain much closer in the unpolarized case. In this favorable distance range, both the level and the spatial variability of DoLP are strongly related to the amount



(a) Median S_0 – Polarized (b) Median S_0 – Unpolarized

Figure 7. Line-by-line evolution of the median total intensity S_0 for different road surface conditions. Left: polarized illumination. Right: unpolarized illumination.



(a) Polarized illumination (b) Unpolarized illumination

Figure 8. Line-by-line angular dispersion of the Angle of Polarization (AoP). Lower dispersion indicates coherent polarization orientation, while higher values reflect increased scattering and surface heterogeneity induced by rainfall.

of water on the surface, so that dry, lightly wet, and heavily wet conditions occupy distinct trajectories as a function of row index.

The median S_0 profiles in Figure 7 further reveal that increasing rainfall intensities produce characteristic changes in the intensity pattern along the road. Under polarized illumination, the growth of S_0 with rain level is relatively smooth and reproducible, reflecting the combined contribution of the wet pavement and the droplets. Under unpolarized illumination, by contrast, S_0 can exhibit strong peaks and large local variations due to glare, which complicates the direct discrimination of surface states from intensity alone.

Finally, the AoP dispersion curves in Figure 8 add complementary information about the spatial coherence of the polarization state. Dry asphalt, with its pronounced roughness and heterogeneous micro-facets, tends to exhibit higher angular dispersion over a wide range of distances. As the surface becomes wet and the rainfall intensity increases, the dispersion decreases in regions where the water film smooths the effective interface and the droplets polarize the light in similar directions. At very high rainfall intensities, more complex patterns may appear due to the dynamic structure of the water layer and volumetric scattering, but the overall behavior remains distinct from the dry case.

Altogether, the line-wise metrics derived from DoLP (median and standard deviation), S_0 (median), and AoP dispersion define a feature space in which the different pavement surface conditions occupy distinct regions, especially under polarized illumination. This suggests that, beyond the descriptive analysis presented here, these metrics could be directly used as input features for automatic classification or risk assessment algorithms dedicated to road surface monitoring under adverse weather and low-light conditions.

5. DISCUSSION AND CONCLUSION

The results presented in this work demonstrate that polarimetric imaging under polarized illumination provides a robust and informative description of wet road surfaces in low-light, rainy conditions. By combining line-wise metrics derived from DoLP, total intensity S_0, and AoP dispersion, it becomes possible to capture both the formation of water films on the pavement and the scattering induced by falling droplets over a wide range of rainfall intensities.

A key outcome of the analysis is that polarized illumination drastically reduces the risk of glare and saturation compared to conventional unpolarized lighting. In the polarized configuration, the growth of S_0 with rainfall intensity remains structured and reproducible, and the specular highlights associated with wet surfaces are better controlled. At the same time, the DoLP and AoP dispersion profiles retain a strong sensitivity to the surface condition, which allows for a reliable discrimination between dry, lightly wet, and heavily wet states, even at mid-range and long distances in the field of view. This combination of reduced glare and preserved polarimetric contrast is particularly beneficial for automotive perception systems that must operate safely in adverse weather.

Another important observation is that polarimetric information remains exploitable at distances where intensity-only cues become less reliable. As the distance from the camera increases, the total intensity tends to decrease and can be more strongly affected by noise and atmospheric attenuation. In contrast, the degree and orientation of polarization still encode meaningful changes in the interaction between light, the water film, and the pavement. The line-wise DoLP and AoP dispersion metrics therefore extend the effective sensing range of the system and help maintain discrimination between surface states farther away from the vehicle.

From an application standpoint, these findings support the use of polarimetric cameras with polarized illumination as a promising sensing modality for advanced driver-assistance systems and autonomous vehicles. The proposed metrics could be directly integrated into classification or risk scoring modules to detect hazardous wet conditions and anticipate loss of adhesion. Future work will focus on extending the experiments to a broader variety of asphalt types and real traffic scenarios, and on coupling the proposed polarimetric descriptors with machine learning models to automatically infer road surface classes and associated risk levels in real time.

ACKNOWLEDGMENTS

This work is supported by the French National Research Agency (ANR) project INARI- ANR-23-CE22-0002.g.

REFERENCES

[1] Rasshofer, R. H., Sporer, M., and Magel, H., "Influences of weather phenomena on automotive laser radar systems," *Advances in Radio Science* **9**, 49–60 (2011).

[2] Roser, M. and Moosmann, F., "Classification of weather situations on single color images," in [*Proceedings of the IEEE Intelligent Vehicles Symposium*], 798–803 (2008).

[3] Nolte, M., Kister, N., and Maurer, M., "Assessment of deep convolutional neural networks for road surface classification," in [*Proceedings of the IEEE International Conference on Intelligent Transportation Systems (ITSC)*], 381–386 (2018).

[4] Wolff, L. B., "Polarization-based material classification from specular reflection," in [*IEEE Transactions on Pattern Analysis and Machine Intelligence*], **12**(11), 1059–1071 (1990).

[5] Schechner, Y. Y., Narasimhan, S. G., and Nayar, S. K., "Polarization-based vision through haze," *Applied Optics* **42**(3), 511–525 (2003).

[6] Tarel, J.-P. and Hautiere, N., "Fast visibility restoration from a single color or gray level image," in [*Proceedings of the IEEE International Conference on Computer Vision (ICCV)*], 2201–2208 (2009).

[7] Yamada, M., Ueda, K., Horiba, I., and Sugie, N., "Discrimination of the road condition toward understanding of vehicle driving environments," *IEEE Transactions on Intelligent Transportation Systems* **2**(1), 26–31 (2002).

[8] Yamada, M., Oshima, T., Ueda, K., Horiba, I., and Yamamoto, S., "A study of the road surface condition detection technique for deployment on a vehicle," *JSAE review* **24**(2), 183–188 (2003).

[9] Casselgren, J., Kutila, M., and Jokela, M., "Slippery road detection by using different methods of polarised light," in [*Advanced Microsystems for Automotive Applications 2012: Smart Systems for Safe, Sustainable and Networked Vehicles*], 207–220, Springer (2012).

[10] Ryu, S.-k., Kim, T., and Bae, E., "Algorithm and experiment for vision-based recognition of road surface conditions using polarization and wavelet transform," *J Emerg Trends Comput Inf Sci* **5**(10), 739–745 (2014).

[11] Blin, R., Ainouz, S., Canu, S., and Meriaudeau, F., "A new multimodal rgb and polarimetric image dataset for road scenes analysis," (2020).

[12] Cerema, "Plateforme pavin brouillard et pluie," (2024).

[13] Lapray, P.-J., Wang, X., Thomas, J.-B., and Gouton, P., "Multispectral filter arrays: Recent advances and practical implementation," *Sensors* **14**(11), 21626–21659 (2014).

[14] Hautière, N., Tarel, J.-P., Lavenant, J., and Aubert, D., "Automatic fog detection and estimation of visibility distance through use of an onboard camera," *Machine Vision and Applications* **17**, 8–20 (april 2006).

[15] Mardia, K. V. and Jupp, P. E., [*Directional statistics*], John Wiley & Sons (2009).